Earth Surface Processes and Landforms
Earth Surf. Process. Landforms **24**, 763–779 (1999)

COMPARISON OF SLOPE ESTIMATES FROM LOW RESOLUTION DEMS: SCALING ISSUES AND A FRACTAL METHOD FOR THEIR SOLUTION

XIAOYANG ZHANG, NICK A. DRAKE*, JOHN WAINWRIGHT AND MARK MULLIGAN
Department of Geography, King's College London, Strand, London WC2R 2LS, UK

Received 19 August 1997; Revised 3 December 1998; Accepted 9 February 1999

ABSTRACT

Five different algorithms for calculating slope from digital elevation models (DEMs) have been compared from regional to global scales. Though different methods produce different results, the most significant outcome is that slope varies inversely with the DEM grid size. Thus, slopes estimated from coarse resolution data can be considered to produce significant underestimates of the true slope. A fractal theory is adapted to solve this problem. The variogram technique for the definition of fractal parameters is demonstrated to provide a relationship between slope and the spatial resolution of measurement. The variation of fractal parameters is discussed at various scales, and a model is developed to estimate the high resolution slope based on the coarse resolution DEM by using fractal parameters. The fractal parameters are estimated from the standard deviation of elevation in a 3×3 window of the DEM to account for local variability in the surface. Standard deviation of elevation is found to be the most invariant property of different scale DEMs of the same area. The model is validated using different resolution DEMs in southern Spain and it is used to estimate the high resolution slope values at global scales based on a coarse resolution DEM. The slopes estimated using the technique outlined are a significant improvement on those estimated directly from the coarse resolution data. Slopes estimated in this way allow the more effective use of available coarse resolution data in regional and global scale modelling studies. Copyright © 1999 John Wiley & Sons, Ltd.

KEY WORDS: slope; DEM resolution; fractal dimension; downscaling; regional to global scale

INTRODUCTION

Topography defines the effects of gravity on the movement of water and sediments in a catchment, therefore digital elevation models (DEMs) play a considerable role in hydrologic simulation, soil-erosion and landscape-evolution modelling. DEMs are used for topographic characterization in a wide variety of scientific, engineering and planning applications. For models of hydrologic and soil-erosion processes, the most important parameters related to DEMs are slope and aspect (Beven and Kirkby, 1979; Band, 1986; Morris and Heerdegen, 1988; Smith *et al.*, 1990; Montgomery and Foufoula–Georgiou, 1993; Zhang and Montgomery, 1994).

The calculation of slope from regional to global scale DEMs is considered here as part of a larger project on runoff and soil-erosion modelling at these scales, in which slope is a key control on the hydrologic and erosion processes simulated (Drake *et al.*, 1995; Zhang *et al.*, 1997). There are three factors which control the effective application of DEMs in this context. First, different results are obtained by different methods of calculating slope and aspect. Some researchers have discussed the influence of various methods of extracting slope (Skidmore, 1989; Jones, 1996). Nevertheless, their studies were carried out only at the catchment or hillslope scale. This study concentrates on global scale DEMs and considers the calculation of

* Correspondence to: Dr N. Drake, Department of Geography, King's College London, Strand, London WC2R 2LS, UK
E-mail: nick.drake@kcl.ac.uk

CCC 0197-9337/99/090763–17 $17.50

slopes using five different methods. Secondly, larger scale DEMs such as those at regional, continental and global scales are more commonly defined by a latitude and longitude (Lat/Lon) projection, where pixel size varies with distance from the equator, influencing the accuracy of slope estimates, especially in high latitude areas.

Thirdly, slopes derived from DEMs vary with the spatial resolution, becoming lower at larger pixel sizes. The issue of the scaling properties of slopes has been studied at various scales. Parsons *et al.* (1997) describe the effects of slope reduction with increasing grid size on predicted overland flow on a hillslope plot in Arizona, with a DEM of 0·5 m base resolution. Using a high resolution (2 m) DEM, Zhang and Montgomery (1994) found that cumulative slope distributions are more sensitive to DEM grid size for steeper catchments than for moderate gradient catchments. Thus the relative elevation constrains the effect of grid size on slope. Hammer *et al.* (1995) compared slope classes from a 10-m and a 30-m resolution DEM with field-measured slope classes in two small catchments. More than 50 per cent of the area was classified into the correct slope classes with the 10-m DEM while only 30 per cent and 21 per cent of the areas were classified correctly with the 30-m DEM. The implication of this study is that high slope values are produced when using high resolution DEMs but slopes are underestimated when using the coarse resolution DEMs. This underestimation can seriously affect the accuracy of hydrological and geomorphological models implemented at coarse resolutions. Quinn *et al.* (1991), Band and Moore (1995) and Zhang and Montgomery (1994) have examined the effect of DEM resolution on the computed distribution of the topographic portion of the hydrological similarity index used in TOPMODEL (Beven and Kirkby, 1979). In these studies, as resolution decreased, the slope values tend to decrease, whereas those of contributing area tend to increase.

A number of authors (e.g. Huang and Turcotte, 1989; Turcotte, 1992; Klinkenberg and Goodchild, 1992) have demonstrated that the topography of the Earth generally exhibits fractal characteristics. This fact implies that there should be a linkage between the observed topography and the scale of observation. Given that slope is the derivative of the local topography, its measurement should therefore also be a function of scale. If so, this linkage may explain some of the difficulties described above of the measurement of slopes from DEMs. Fractal techniques are therefore potentially useful in providing better estimates of the local slope using only coarse resolution data.

Although the increasing availability of DEMs allows rapid analysis of slopes from small catchments to regional and global scales, little attention has been focused on the problems associated with calculating accurate slopes from regional and global scale DEMs. Therefore the objectives of this study are:

(1) to compare the slopes derived from five different methods and two different co-ordinate systems of DEMs at various scales;
(2) to investigate the relationship between slope and topographic fractal properties;
(3) To develop a uniformly applicable method of estimating high resolution slopes from coarse scale DEMs using these topographic fractal properties;
(4) to validate this method using high resolution DEMs.

SELECTED DEMS

In order to accomplish these aims, several different DEMs were employed (Figure 1). Three global scale DEMs were used. These are the 30″ resolution DEM from the EROS Data Centre (http://edcwww.cr.usgs.gov/landdaac), and the 5′ and 10′ resolution DEMs from the Terrain Base world wide digital terrain data CD-ROM provided by the National Geophysical Data Center, Boulder, Colorado, USA. The area selected for this study is in Eurasia and northern Africa between 7·5°S–62·0°N and 19·0°W–128·2°E. All DEMs are supplied on the Lat/Lon co-ordinate system. The grid sizes of these three DEMs range from 435 m × 926·66 m to 926·64 m × 926·64 m in the 30″ DEM, 4350·3 m × 9266·4 m to 9266·4 m × 9266·4 m in the 5′ DEM and 8700·6 m × 18 532·8 m to 18 532·8 m × 18 532·8 m in the 10′ DEM. A sub-area (about $1{\cdot}332 \times 10^7$ km^2) of the 30″ DEM for eastern Asia between 20–40°N and 70·5–123·9°E was selected for intensive study as the region includes nearly all the different types of topography in the world including the highest mountains

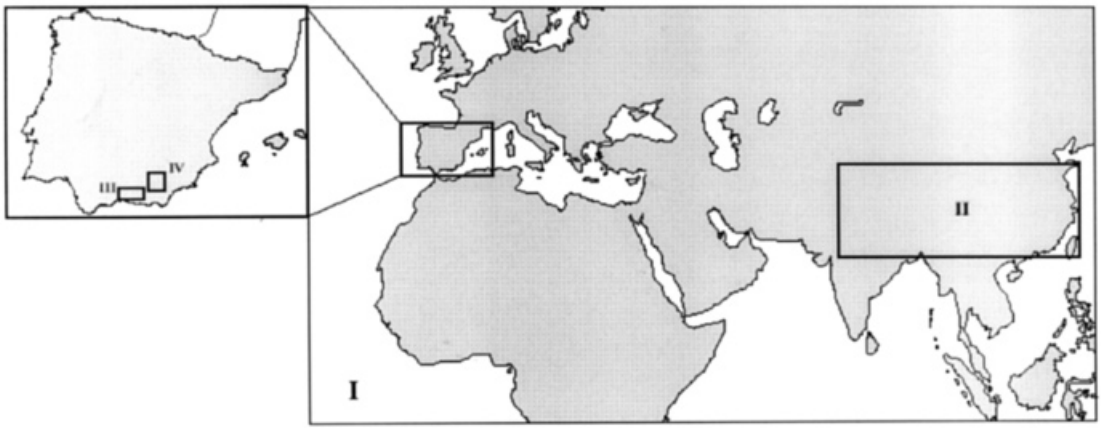

Figure 1. Map showing the locations of the DEMs used in the analyses. I, Global scale DEM covering the area 7·5°S–62°N, 19°W–128·2°E; II, area of eastern Asia from 20–40°N, 70·5°–123·9°E extracted from the global scale DEM; III, Guadalfeo Basin; IV, Guadalentín Basin, including the Rambla del Chortal

(Himalayas), the highest plateau (Tibetan), hills, basins, plains and coasts. This region represents the most complicated land surface on Earth.

To provide information about slope values calculated at much finer resolutions, a second series of three pre-existing high resolution DEMs from southeastern Spain was selected (Figure 1). This region is again dominated by complex topography, albeit not encompassing the range found in the eastern Asia DEM. Three high resolution DEMs supplied on a Universal Transverse Mercator (UTM) projection are used.

(1) The Rambla del Chortal DEM, which is of a small catchment of 15·26 km^2 with a pixel size of 20 m. The contours were digitized at King's College London from the 1:50 000 Mapa Militar de España, and interpolated using the GRASS GIS.
(2) The Guadalentín Basin DEM with a pixel size of 30 m and an area of 3142·9 km^2. The DEM was interpolated in ARC/INFO using the TIN module from digitized contours of the 1:50 000 Mapa Militar de España.
(3) The Guadalfeo Basin DEM which is extracted from the Sierra Nevada DEM with a grid size of 200 m and an area of 1677·7 km^2.

In order to analyse the scaling properties of slope, the spatial resolution of each of the above-mentioned DEM data sets was reduced by averaging. This operation is reasonable under the assumption that digital elevation data at a given resolution (grid size) can be interpreted as averages over an area surrounding the point at which elevation is reported (Helmlinger *et al.* 1993). Hence DEMs with various resolutions were created. The resulting resolutions are 30″, 1′, 2′, 4′, 8′, 16′ and 32′ in eastern Asia; 30 m, 60 m, 120 m, 240 m, 480 m, 960 m and 1920 m in the Guadalentín Basin; 20 m, 40 m, 80 m, 160 m, 320 m, 640 m and 1280 m in the Rambla del Chortal; and 200 m and 2000 m in the Guadalfeo Basin.

ALGORITHMS FOR ESTIMATING SLOPE

To calculate slope from a regularly gridded DEM, an assumption must be made about the way the grid points represent the land surface. It is common to use a 3 × 3 pixel window around a particular point to approximate this surface since local slope is a function of nearest-neighbour pixels. Different assumptions of shape within this window will provide different results (Skidmore, 1989; Jones, 1996). Five different methods are used

here for estimating the local surface within the window. In the following discussion, the terms S_1 to S_5 (m m^{-1}) will be used to refer to the slopes calculated by different methods.

Method 1 Slope is defined as the direction of the maximum drop from centre pixel to its eight nearest neighbours:

$$S_1 \max[(Z_{i,j} - Z_{i-1,j-1})/\Delta X_1, (Z_{i,j} - Z_{i-1,j})/\Delta X_2, \ldots, (Z_{i,j} - Z_{i+1,j+1})/\Delta X_8] \quad (1)$$

where Z is the elevation of the DEM at a given point (m); i and j index the pixel locations; and ΔX_1–ΔX_8 are the distances (m) between the central pixel and the eight neighbouring pixels. This technique is also known as the steepest descent or D8 method.

The following four methods calculate the slope as a function of the slope along the X and Y directions of the DEM. The slope from a fitted surface can be calculated using the following equation:

$$S_n = \sqrt{S_x{}^2 + S_y{}^2} \quad (2)$$

where S_x and S_y are the slope in the X and Y directions respectively (m m^{-1}) and n relates to the method used to derive S_x and S_y.

Method 2 Using a linear regression model proposed by Travis *et al.* (1975) and reported by Evans (1980), the local topographic surface in a 3×3 window is approximated by:

$$Z = aX + bY + c + \varepsilon \quad (3)$$

where X and Y are distances along the DEM coordinates (m); a, b and c are constants; and ϵ is error. Therefore, $S_x = a$ and $S_y = b$.

Method 3 A full quadratic surface in a 3×3 window is given by the equation (Evans, 1980):

$$Z = aX^2 + bY^2 + cXY + dX + eY + f + \varepsilon \quad (4)$$

where a, b, c, d, e and f are constants. Hence,

$$S_x = 2aX + cY + d \quad (4a)$$

and

$$S_y = 2bY + cY + e \quad (4b)$$

Method 4 Assuming that the chosen surface does pass exactly through the nine submatrix elevations in a 3×3 window, the appropriate surface is produced by the partial quadratic equation (Zevenbergen and Thorne, 1987):

$$Z = aX^2Y^2 + bX^2Y + cXY^2 + dX^2 + eY^2 + fXY + gX + hY + k \quad (5)$$

where a to h and k are constants. Therefore,

$$S_x = 2aXY^2 + 2bXY + cY^2 + 2dX + fY + g \quad (5a)$$

and

$$S_x = 2aX^2Y + bX^2 + 2cXY + 2eY + fX + h \tag{5b}$$

The nine parameters can be determined from the nine elevations of the 3×3 submatrix by Lagrange polynomials.

Method 5 The third-order finite difference method for calculating gradient and aspect proposed by Horn (1981) is:

$$\begin{aligned} S_x &= [(Z_{i+1,j+1} + 2Z_{i+1,j} + Z_{i+1,j-1}) - (Z_{i-1,j+1} + 2Z_{i-1,j} + Z_{i-1,j-1})]/8\Delta X \\ S_y &= [(Z_{i+1,j+1} + 2Z_{i,j+1} + Z_{i-1,j+1}) - (Z_{i+1,j-1} + 2Z_{i,j-1} + Z_{i-1,j-1})]/8\Delta Y \end{aligned} \tag{6}$$

where ΔX and ΔY are the distances (m) between the pixels in the X and Y directions respectively.

Calculating slope from high resolution DEMs using the above-mentioned methods is straightforward because pixel size is uniform in the UTM grid. However, the coarse resolution DEMs are provided on a Lat/Lon system which can affect the accuracy of the resultant slopes in high latitude areas, as noted above. Although the Lat/Lon projection can be converted to a UTM projection before the slope calculation, there are several problems which will affect the accuracy of the results at the global scale. First, the global data have to be divided into a large number of UTM zones. Secondly, the original data have to be interpolated to make each pixel the same size. Thirdly, the UTM projection needs to be converted back to the Lat/Lon system again to match other data for modelling. However, the boundary-slope values of neighbouring zones cannot be matched because there is no accurate slope around the edge of the DEM. Fourthly, this process (Lat/Lon–UTM–Lat/Lon) not only results in the loss of some information but is also time consuming.

A method of computing slope directly from DEMs on the Lat/Lon system has therefore been developed to overcome these problems. In a DEM with a UTM projection, the grid size and the lengths in both S–N and E–W directions for each grid cell are the same. In the Lat/Lon system, however, the pixel size is larger in low than in high latitudes, and the distance between a central pixel and each neighbouring pixel is different. Hence, the different distance between grid cells has to be taken into account in global scale DEMs using the Lat/Lon projection. The distances in each direction can be calculated by using following equations.

The arc distance (X_{ew}) along the parallel of latitude ϕ(E–W) (m) is:

$$X_{ew} = R\delta \cos\phi \tag{7}$$

where ϕ is the latitude (degrees), δ is the difference of longitude (degrees of arc) and R is the radius of the Earth ($6{\cdot}3711 \times 10^6$ m).

The length of the arc (Y_{sn}) in a meridian (S–N) (m) is:

$$Y_{sn} = R\Delta\phi \tag{8}$$

where $\Delta\phi$ is difference of latitude between two points (degrees of arc).

The length between any two points on a diagonal (P_{XY}) (m) is:

$$P_{XY} = R\phi \tag{9}$$

where

$$\cos\phi = \sin\phi_a \sin\phi_b + \cos\phi_a \cos\phi_b \cos\delta \tag{10}$$

where ϕ_a and ϕ_b are the latitudes (degrees) at the two points and δ is the difference between longitudes (degrees) of the two points.

Thus to evaluate slopes on a Lat/Lon grid, the distance between pixels is calculated using equations 8, 9 and 10. Following this, the slopes are calculated using the different methods outlined above for the selected DEMs. The difference between each two sets of slope values is termed the residual slope and the average value of their root-mean square (RMS) error is calculated in order to determine the magnitude of the differences between the different methods.

COMPARISON OF SLOPES DERIVED FROM DIFFERENT METHODS

The RMS error of percentage slope in eastern Asia is shown in Table I. The RMS error between methods 2 and 3 is zero. These two methods produce exactly the same slope because the tangent plane in method 2 is parallel with the surface of method 3. The RMS error between any two different methods is larger for slopes derived from high resolution DEMs than from low resolution DEMs because the slope values from the coarser resolution DEM become smaller. At the same resolution slopes, the order of RMS values is RMS1,2 > RMS1,5 > RMS1,4 > RMS2,4 > RMS4,5 > RMS2,5, where 1, 2 (or 3), 4 and 5 are the method numbers.

The slope also differs among the various methods. The average slopes at every spatial scale are between 0·53 and 0·79 times higher using method 1 when compared with the other methods (Table II). The cumulative frequency distribution of the various methods of calculating slope also shows that the range of slopes is much larger in method 1 than in the other surface-fitting methods (Figure 2). The slope values from method 4 are the largest among the four surface-fitting methods. Method 5 generates very similar slope values to method 2 (or 3) because of the similarities in these methods. Thus method 1 produces the largest slope, followed by method 4, method 5 and method 2 (or 3) in turn.

The spatial distribution of the different RMS errors shows that the largest difference in slope is in mountainous areas at all DEM resolutions. In the eastern Asia DEM the average RMS error of the slope in mountainous regions is about three times that in hills, and about 23 times that in plains and basins (Table III). The RMS error is therefore sensitive to the topographic environment. The more changeable the elevation, the larger the RMS will be. However, the relative errors in slope (the difference in the values estimated using the two different techniques divided by their average) show the opposite trend, being higher in the plains and basins than in either the hills or mountainous areas. This result suggests that for processes where small slope angles are important, for example flow routing over flat terrain, the resultant errors from calculating the slopes using coarse resolution data are also significant in areas of low slope.

Although the calculated slopes vary between different methods, these variations are small when compared to the changes in slope caused by changing the resolution of the DEM. High resolution DEMs produce high slopes while low slopes are derived from coarse resolution DEMs even though the area is exactly the same (Table II). For example, using method 1 the average slope for the eastern Asia DEM at 32′ resolution is only 6·9 per cent of the slope at 30″ resolution, and for the Guadalentín DEM, the average slope at 240 m resolution is only 63 per cent of the slope at the original 30 m resolution. As the high resolution DEM is a more accurate representation of the real surface, it is clear that the low resolution DEM underestimates the local slope. This reduction in slope results in difficulties in the application of slope derived directly from coarse scale DEMs. For the development of global scale hydrologic, soil-erosion and landscape-evolution models, it is necessary to overcome this problem. One way of doing this is to estimate the average value of slope in the high resolution DEM using only the coarse resolution DEM since only the coarse resolution DEMs are available for large parts of the Earth. Given that topography is generally fractal (Huang and Turcotte, 1979), it is expected that the topography represented by the DEM will be a function of the DEM pixel size. Hence, fractal methods might be a useful tool to solve this scaling problem.

To demonstrate that the decrease in slope with increasing pixel size is not an artefact of the averaging technique used to generate the coarse resolution DEMs, a second series of DEMs was generated for the Guadalentín basin. These DEMs were constructed by subsampling the 30-m DEM at fixed intervals, taking every second pixel to generate a 60-m resolution DEM, every fourth pixel to generate a 120-m resolution

Table I. RMS error of percentage slope for comparison of different slope-estimation techniques for different resolution DEMs of the same area in eastern Asia

DEM	30′					1′					2′					4′					8′					16′					32′				
Mehod	S_1	S_2	S_3	S_4	S_5	S_1	S_2	S_3	S_4	S_5	S_1	S_2	S_3	S_4	S_5	S_1	S_2	S_3	S_4	S_5	S_1	S_2	S_3	S_4	S_5	S_1	S_2	S_3	S_4	S_5	S_1	S_2	S_3	S_4	S_5
S_1	0	9·17	9·17	8·04	8·90	0	6·84	6·84	5·96	6·64	0	4·60	4·64	4·02	4·51	0	2·91	2·91	2·52	2·83	0	1·70	1·70	1·48	1·66	0	0·90	0·90	0·81	0·88	0	0·55	0·55	0·53	0·55
S_2		0	0	3·21	0·79		0	0	2·42	0·59		0	0	1·64	0·40		0	0	1·03	0·25		0	0	0·60	0·15		0	0	0·31	0·09		0	0	0·17	0·06
S_3			0	3·21	0·79			0	2·42	0·59			0	1·64	0·40			0	1·03	0·25			0	0·60	0·15			0	0·31	0·09			0	0·17	0·06
S_4				0	2·48				0	1·87				0	1·27				0	0·80				0	0·47				0	0·25				0	0·14

Table II. Average percentage slope values calculated for the eastern Asia DEM using the different methods discussed in the text at various scales

Grid size	S_1 (%)	S_3 (%)	S_4 (%)	S_5 (%)
30″	12·429	7·171	8·139	7·348
1′	8·652	4·703	5·447	4·829
2′	5·667	2·939	3·453	3·023
4′	3·527	1·752	2·090	1·805
8′	2·108	1·023	1·221	1·051
16′	1·266	0·658	0·754	0·671
32′	0·862	0·480	0·524	0·485

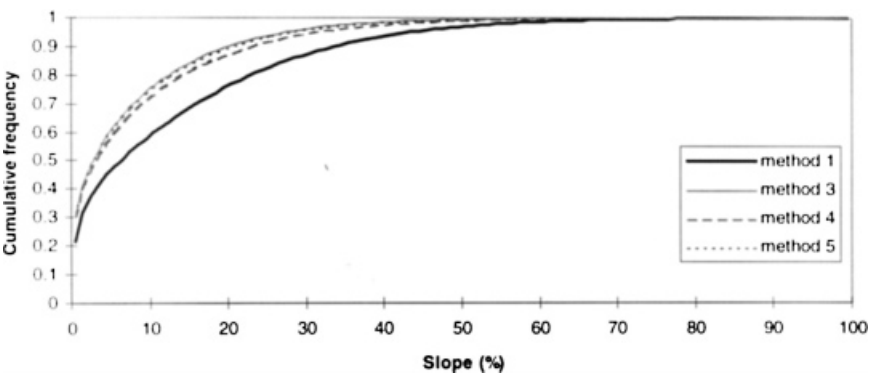

Figure 2. Cumulative frequency distribution of slopes calculated from the 30″ DEM for eastern Asia using various methods

Table III. RMS error comparing the different methods of estimating slope discussed in the text in different landscapes of eastern Asia

	Mountain	Hill	Plain and basin
RMS S_1–S_2	4·01	1·33	0·17
RMS S_1–S_4	12·60	4·20	0·55
RMS S_1–S_5	0·98	0·33	0·04
RMS S_2–S_4	10·28	3·45	0·16
RMS S_2–S_5	3·10	1·03	0·13
RMS S_4–S_5	12·15	4·06	0·53

Table IV. Comparison of average slope estimates for coarse resolution DEMs derived by pixel thinning or pixel aggregation, based on the Guadalentín DEM using the S_1 method. The average slope for the original, 30 m resolution DEM is also shown for comparison

	DEM resolution			
	30 m	60 m	120 m	240 m
Slope (%) from pixel thinning	15·42	14·49	12·62	10·26
Slope (%) from pixel aggregation		14·21	12·11	9·66
RMS error	-	0·008	0·023	0·045

DEM, every eighth pixel to generate a 240-m resolution DEM. DEMs constructed in this way by pixel thinning are analogous to the generation of different resolution DEMs from the same original base contour data, by the superimposition of grids of different sizes. Slopes derived from the DEMs produced by pixel thinning show the same general trend as those derived from pixel aggregation, although the decrease in slope is not as large (Table IV). Thus, it can be concluded that the trends observed in this paper are independent of the method used to generate the coarse resolution DEM.

SLOPE AND TOPOGRAPHIC FRACTAL PROPERTIES

A fractal is an object whose shape is independent of the scale at which it is regarded (Turcotte, 1992). Huang and Turcotte (1989) indicated the Earth's topography generally obeys fractal statistics and the mean fractal dimension (D) is 1·52. In the natural environment, most landscapes can be considered to be fractal (Moore *et al.*, 1993), although there are some limitations. Andrle and Abrahams (1989), for example, found that talus slope surfaces are not self-similar and therefore the fractal properties may break down at very small scales.

A variety of methods have been proposed to determine the fractal dimension of topography (Klinkenberg and Goodchild, 1992; see also Aviles *et al.* (1987), Goodchild (1982), Håkanson (1978), Kent and Wong (1982), Mandebrot (1982), Russ (1993) and Shelberg *et al.* (1982) for examples of the techniques that can be used). The essence of the variogram technique is that the statistical variation of the elevations between samples varies with the distance between them. The independent variable is the distance between pairs of points while the dependent variable is the variance of the differences in the data values for all samples a given distance apart (Klinkenberg and Goodchild, 1992). This method can be used to calculate the fractal dimension in a region when the log of distance between samples is regressed against the log of the mean-squared difference in the elevations for that distance (Cressie and Hawkins, 1980; Klinkenberg and Goodchild, 1992).

According to the variogram technique, the relationship between the elevations of two points and their distance can be converted to the following formula:

$$(Z_p - Z_q)^2 = kd^{4-2D} \tag{11}$$

so that:

$$\frac{Z_p - Z_q}{d} = \alpha d^{1-D} \tag{12}$$

where Z_p and Z_q are the elevations (m) at points p and q, d is the distance (m) between p and q, k and $\alpha = \pm k^{0.5}$ are constants and D is the fractal dimension. The value $(Z_p - Z_q)/d$ is actually the surface slope. It can be assumed, therefore, that the percentage slope S is related to its corresponding scale (grid size) d by the

equation:

$$S = \alpha d^{1-D} \tag{13}$$

This relationship implies that if topography is fractal, then slope will also be a function of the scale of measurement. However, it is not reasonable to talk of 'fractal slopes' as the initial topography is not differentiable. When using topographic fractal properties to provide better slope estimates from coarse resolution data, we will refer to scaled slope in the following discussion.

It is interesting to note the similarity between Equation 13 and the Korcak relationship of a fractal set (Russ, 1993). This equation describes the number of islands in the Korcak group with coastlines of a specific length, and can be defined as:

$$N = \beta t^{1-D} \tag{14}$$

where N is the number of objects with the linear dimension t, D is the fractal dimension and β is a coefficient of proportionality. Many objects on the surface of the Earth can be described using this equation.

Using topographic fractal properties to scale slope

The results presented above have demonstrated that the general trends of slopes calculated from different resolution data are the same regardless of the techniques used to calculate slope. Therefore, only slopes calculated using method 1 and method 4 have been used to study their relationship with topographic fractal properties. Using the eastern Asia DEM, the average scaled slope derived from method 1 is:

$$S = 1166 \cdot 24\ d^{-0{\cdot}66149} \tag{15}$$

with $r^2 = 0{\cdot}997$, $F = 198{\cdot}9$ and $p < 1 \times 10^{-5}$.

Thus the average slope values in a DEM can be estimated at different resolutions when using the slope scaling Equation 15. However, it is impossible to predict the spatial patterns of slopes, due to the following problems:

(1) the single value of the fractal dimension for the whole DEM; and
(2) the coefficient in the fractal topographic slope equation is considered to be a constant and little attention has been paid to its variation with different landscapes.

It is reasonable to suppose that different kinds of terrain might have characteristic topography that can be expressed in terms of different values of α and D (Barenblatt *et al.*, 1984; Fox and Hayes, 1985; Klinkenberg, 1992). It is therefore logical to assume that there is a set of different scaled slopes when a DEM is divided into several small subregions. Thus for calculating the local fractal properties and scaled slope it is assumed that:

(1) the smallest subarea (window) is composed of 3×3 pixels;
(2) the slope in each 3×3 window changes with scale;
(3) the coefficient α and fractal dimension D of topography remain stable in the same 3×3 window.

In the light of these assumptions, the eastern Asia and Guadalentín Basin DEMs are degraded to a coarse spatial resolution by pixel averaging and divided into a series of 3×3 pixel subareas. The subareas are about 27 361·8 km^2 in the 32′ eastern Asia DEM and 33·18 km^2 in the 1920 m DEM of southern Spain. The high resolution data are used to calculate the fractal parameters for these subareas and it is found that both α and D vary considerably (Table V). The value of D, for example, ranges from 1·03 to 1·48 (average 1·27) in the Guadalentín Basin, and from 1·06 to ·1·96 (average 1·61) in eastern Asia when the slopes are computed using method 1. Furthermore, α is far from constant, with values ranging from 0·59 to 2023·1.

Table V. The variation of fractal parameters calculated using the semi-variogram technique based on the eastern Asia and the Guadalentín Basin DEMs

Method of calculating slope	Statistics	α	D
S_1	Average	2023·10	1·55
	Maximum	31193·74	1·96
	Minimum	0·59	1·03
	Standard deviation	3910·06	0·22
S_4	Average	1959·11	1·60
	Maximum	29330·11	1·99
	Minimum	1·26	1·02
	Standard deviation	3715·91	0·22

Table VI. Statistics of the relationship between the standard deviation of elevation and the scale of the DEM. The subscripts 0·5′–32′ and 30 m–1,920 m indicate the different pixel sizes

Location	Regression equation	r^2	F	p
Eastern Asia	$\sigma_{0.5'} = 71{\cdot}4061 + 1{\cdot}0047\sigma_{32'}$	0·995	3996·4	<0·0001
	$\sigma_{1'} = 68{\cdot}3562 + 1{\cdot}0047\sigma_{32'}$	0·995	4415·9	<0·0001
	$\sigma_{2'} = 63{\cdot}1411 + 1{\cdot}0043\sigma_{32'}$	0·996	5421·0	<0·0001
	$\sigma_{4'} = 54{\cdot}6689 + 1{\cdot}0034\sigma_{32'}$	0·997	7887·7	<0·0001
	$\sigma_{8'} = 41{\cdot}5627 + 1{\cdot}0025\sigma_{32'}$	0·999	15808·8	<0·0001
	$\sigma_{16'} = 23{\cdot}02725 + 1{\cdot}0005\sigma_{32'}$	0·9996	56385·9	<0·0001
Guadalentín	$\sigma_{30m} = 3{\cdot}5419 + 1{\cdot}0414\sigma_{1920m}$	0·995	3375·83	<0·0001

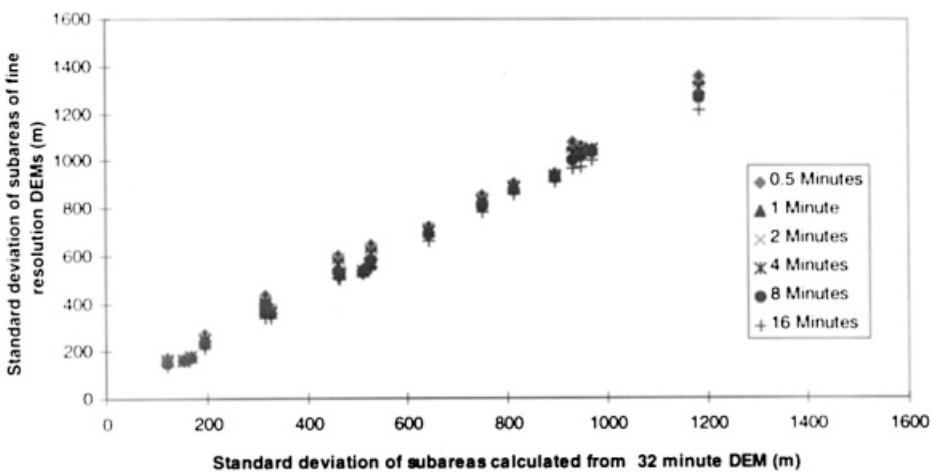

Figure 3. The relationship between the standard deviation of elevation and the grid resolution for the eastern Asia DEM

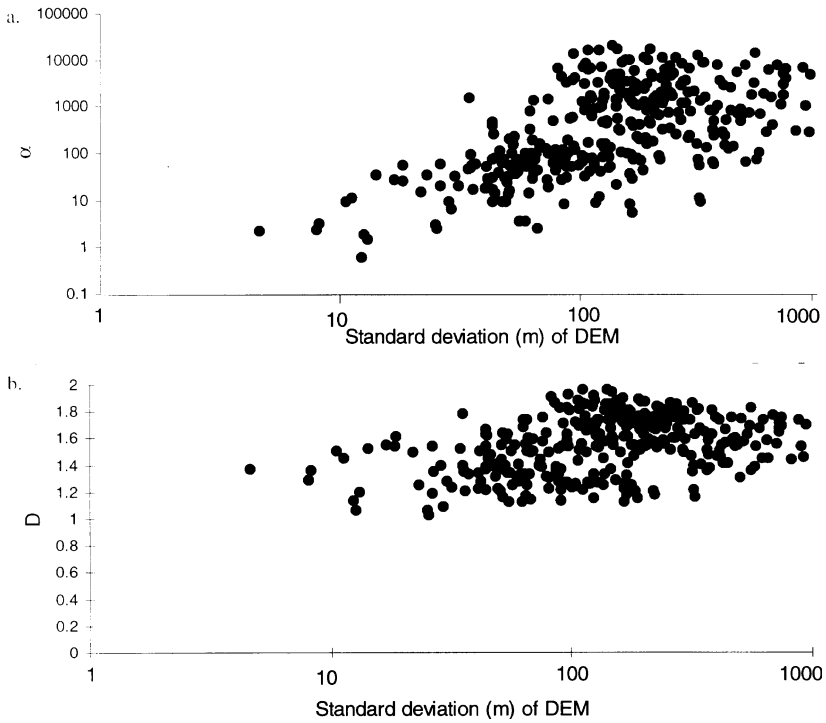

Figure 4. The relationship between standard deviation of elevation and the topographic fractal parameters: (a) fractal coefficient α; and (b) topographic fractal dimension D

Estimating scaling parameters for calculation of high resolution slopes from coarse resolution data

In order to use Equation 13 to calculate local slope at a specified finer scale (d) it is necessary to develop a method for calculating the local fractal parameters from the coarse resolution data. The slope is determined by the difference in elevation between two points a given distance apart. The distance can be represented by grid size in a DEM and the roughness of relief in an area can be substituted by the standard deviation (σ) of the elevation.

When the standard deviations in the subareas of various resolution DEMs are compared, it is seen that there is a large variation in the standard deviation between different subareas but only a slight decrease from high resolution to low resolution in the same subarea (Table VI, Figure 3). The coefficient α and the fractal dimension D vary in different subareas; however, they are mainly controlled by the standard deviation of the elevations. Significant relationships are found between D and α and σ when the scaling coefficients derived from eastern Asia and southeast Spain are plotted against the corresponding standard deviation of elevation (Figure 4). When the slopes are calculated by method 1, the regression equations are:

$$\alpha = 0 \cdot 33733\ \sigma^{1 \cdot 4004} \tag{16}$$

with $r^2 = 0{\cdot}34$, $n = 347$, $F = 177{\cdot}29$ and $p < 1 \times 10^{-5}$; and:

$$D = 1 \cdot 13589 + 0 \cdot 08452 \ln \sigma \tag{17}$$

with $r^2 = 0{\cdot}135$, $n = 347$, $F = 53{\cdot}8757$ and $p < 1 \times 10^{-5}$.

For slopes derived from method 4, the scaling parameters can be estimated by the following equations:

$$\alpha = 0 \cdot 3047\ \sigma^{1 \cdot 4106} \tag{18}$$

Table VII. Validation of the scaled slope method based on slope-estimation methods S_1 and S_4, using the high resolution DEM estimate as the best estimate of the real slope. The statistics for the unscaled slope estimates are shown for comparison

		Method S_1			Method S_4		
Location	Statistics	High resolution slope	Scaled slope	Unscaled slope	High resolution slope	Scaled slope	Unscaled slope
Guadalentín	Average	19·11	17·26	8·94	15·19	13·79	5·83
Basin	σ	13·30	14·70	8·74	11·32	11·95	5·78
	Min.	0	0·29	0·21	0	0·22	0·05
	Max.	81·27	107·40	46·08	71·27	87·84	38·76
Guadalfeo	Average	30·04	26·56	14·66	22·74	19·80	10·20
Basin	σ	10·92	10·61	11·23	8·48	8·10	8·94
	Min.	3·41	6·66	3·45	2·69	4·81	1·27
	Max.	65·48	55·71	32·0	50·42	42·21	27·36

773with $r^2 = 0{\cdot}334$, $n = 354$, $F = 177{\cdot}99$ and $p < 1 \times 10^{-5}$; and:

$$D = 1 \cdot 19324 + 0 \cdot 082507 \ln \sigma \tag{19}$$

with $r^2 = 0{\cdot}122$, $n = 373$, $F = 48{\cdot}78$ and $p < 1 \times 10^{-5}$.

Although the scaling parameters are slightly different between methods 1 and 4, the value of α in both methods is more sensitive than fractal dimension D to the standard deviation of elevation. The value of α varies from 0 to 10^4 while D ranges from 1·02 for completely smooth surfaces to 1·99 for very irregular surfaces. A wide range of fractal dimension values has also been reported for topographical surfaces (Turcotte, 1992) and for remotely sensed images (De Jong and Burrough, 1995). Thus to estimate scaled slope S, α and D can be estimated from Equations 16 and 17 or 18 and 19 and then S can be estimated from Equation 13 at a specified scale (d).

Validation of scaled slope properties

Two scales of DEM are applied to validate the scaled slope in two areas. First, the Guadalfeo Basin DEM with a resolution of 200 m is used to validate a coarse scale DEM with a pixel size of 2000 m that was created by averaging. Secondly, the Guadalentín Basin DEM with a spatial resolution of 30 m is compared to the corresponding region of the global 30″ DEM. In order to match the pixels in the 30″ DEM to the 30 m DEM, the 30″ DEM is converted to the UTM projection with nearest-neighbour resampling. In each subarea, the average slope computed from the high resolution DEM is taken as the best estimate of the real slope at the pixel size of the coarse resolution DEM, whereas predicted slope at the high resolution is estimated from the coarse resolution DEM using the scaled slope technique.

When this method of validation is applied, the predicted slope (scaled slope) is very similar to the real slope whereas the slopes are very different when calculated from high and low resolution DEMs using methods 1 and 4 (Table VII, Figure 5). The RMS error is 3·92 (relative error 9·7 per cent) for method 1 and 6·29 (relative error 9·2 per cent) for method 4 in Guadalentín Basin and is 8·63 (relative error 11·6 per cent) and 5·34 (relative error 12·9 per cent) in the Guadalfeo Basin. Errors are unlikely to be due to the fact that different resolution DEMs were compiled in different ways with different accuracies (as was the case with the comparison of the Guadelentín and the 30″ DEM), because this comparison produced the lower RMS errors.

Limitations of the scaled slope method

The technique presented above seems to break down at certain scales in certain topographic environments. In some mountainous regions of eastern Asia, the average slope decreases with the grid size from 30″ to 8′

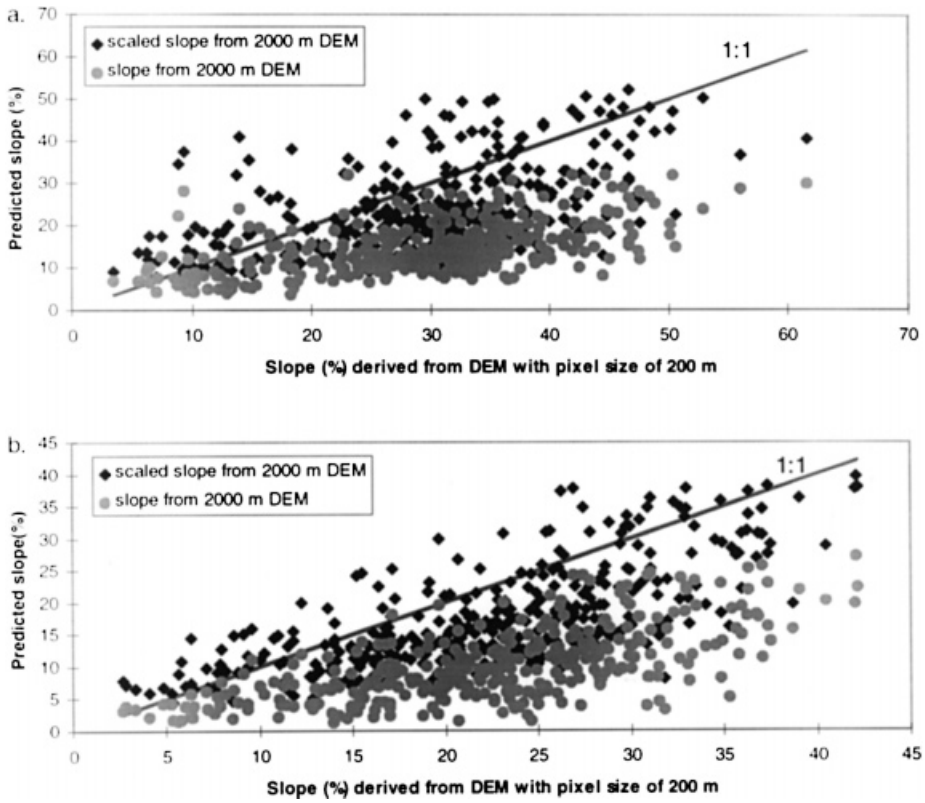

Figure 5. Comparison of unscaled slope and scaled slope using the Guadalfeo Basin 200 m DEM: (a) slopes calculated using method S1 (Equation 1); (b) slope calculated using method S4 (Equations 2 and 5)

(i.e. resolution is reduced by 16×). Conversely, it increases again when the grid size equals 16′ (resolution reduced by 32×), then decreases with greater pixel sizes. Thus the scaling properties of slope are affected in very coarse resolution DEMs if the relative elevation changes considerably within a pixel, such as in locations where very high mountains are separated by very deep valleys. This problem seems to arise because, in these areas, spatial averaging makes high slopes lower, but also low slopes higher. As a result, in 6·0 per cent of the eastern Asia DEM (mainly in the Himalayan mountains) the fractal scaling properties of slope are lost. The same loss also occurs in 4·3 per cent of the Guadalentín Basin DEM when the spatial resolution is reduced to a level where coarse resolution pixel size is more than 32 times larger than that in the high resolution DEM. The implications of these results are that the scaling of slope is sensitive to the relative elevation and also that the scaling properties of slope apply for limited areas over limited ranges of scale, as found at fine scales by Andrle and Abrahams (1989). Different processes forming the slopes at different scales may account for the these difficulties.

Scaling slopes at the global scale

When the 5′ DEM is used to estimate the spatial distribution of the topographic fractal properties it is found that the fractal dimension varies between 1·6 and 1·9 in the high mountains, between 1·4 and 1·6 in hilly areas, and between 1·1 and 1·4 in plains or basins (Figure 6a). The coefficient α ranges from 0 to 5000 although it is less than 20 in 37 per cent of the region and it has a similar spatial distribution to the fractal dimension (Figure 6b). A value of d of 30 m was then used to calculate the scaled slope using Equation 13, assuming that a 30 m pixel size can represent the real hillslope at the global scale. It is found that the average slope values estimated from the scaling properties range from 0 to 300 per cent and they are less than 10 per

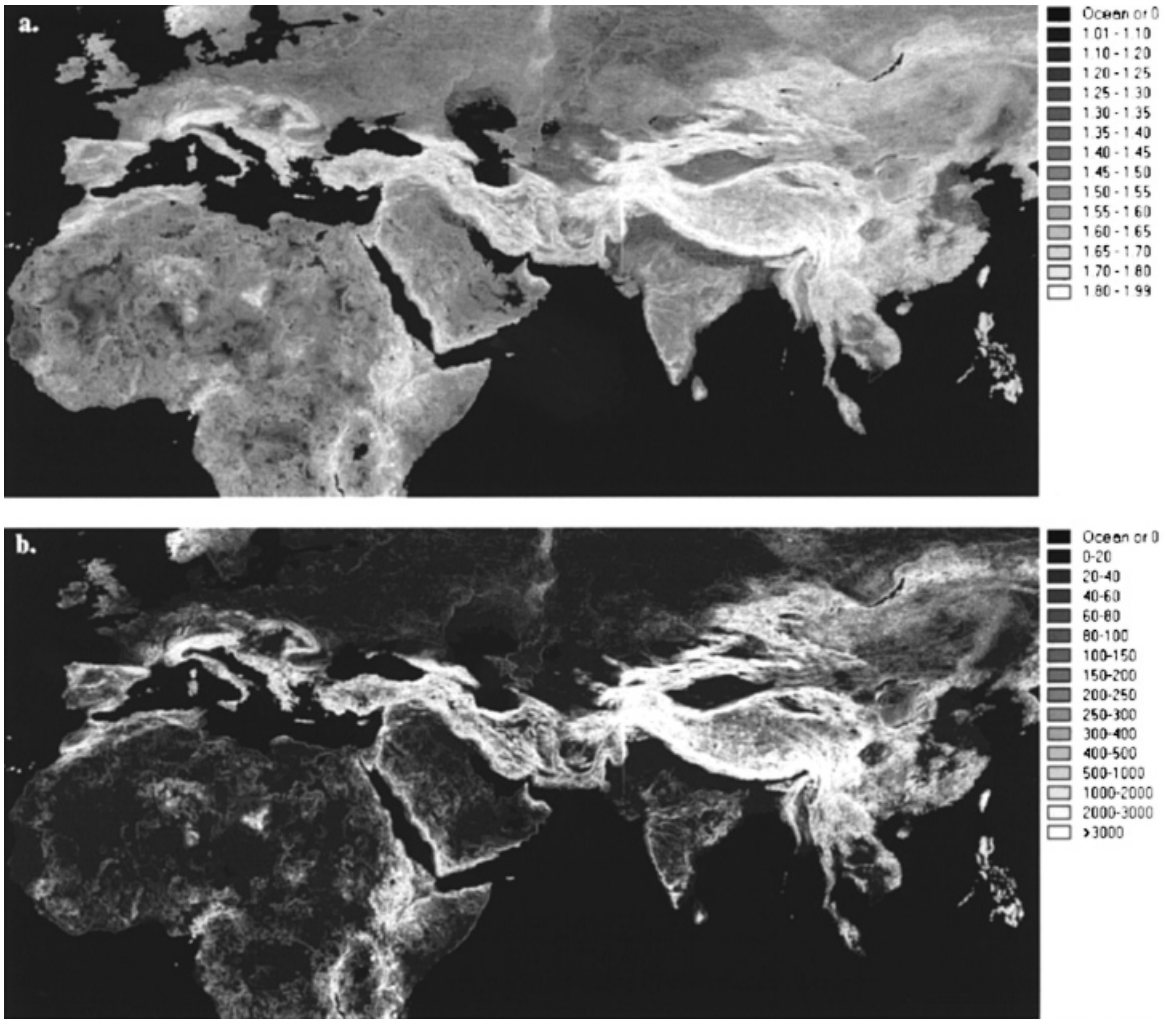

Figure 6. Fractal parameters for the Eurasia and northern Africa region DEM: (a) fractal dimension D; (b) fractal coefficient α

cent in 51 per cent of the area (Figure 7a). In contrast, all the slope values are less than 30 per cent and range between 0 and 2 per cent in 86 per cent of this area when slope is computed directly from the 5′ DEM (Figure 7b). The average percentage slope in Eurasia and north Africa is 1·27 for the 10′ DEM, 1·41 for the 5′ DEM, 4·87 for the 30″ DEM and 25·69 for the scaled slope. Furthermore, the cumulative frequency distribution of slope (Figure 8) demonstrates that the range of slope values is largest with the 30 m scaled slope, and decreases with increasing pixel size.

CONCLUSIONS

Five different algorithms for calculating slopes have been compared at various scales. The maximum drop within a 3×3 pixel window, which is applied by most GIS software, not surprisingly produces a larger slope than surface fitting methods at the various resolutions of the DEMs. Unfortunately, it is not possible to measure the actual slope over a large area so that it is impossible to demonstrate which method is best. Land-surface type plays an important role in the application of slope calculation. The maximum difference in the slopes derived from the various methods is found in mountainous areas, followed by hills and then plains and basins.

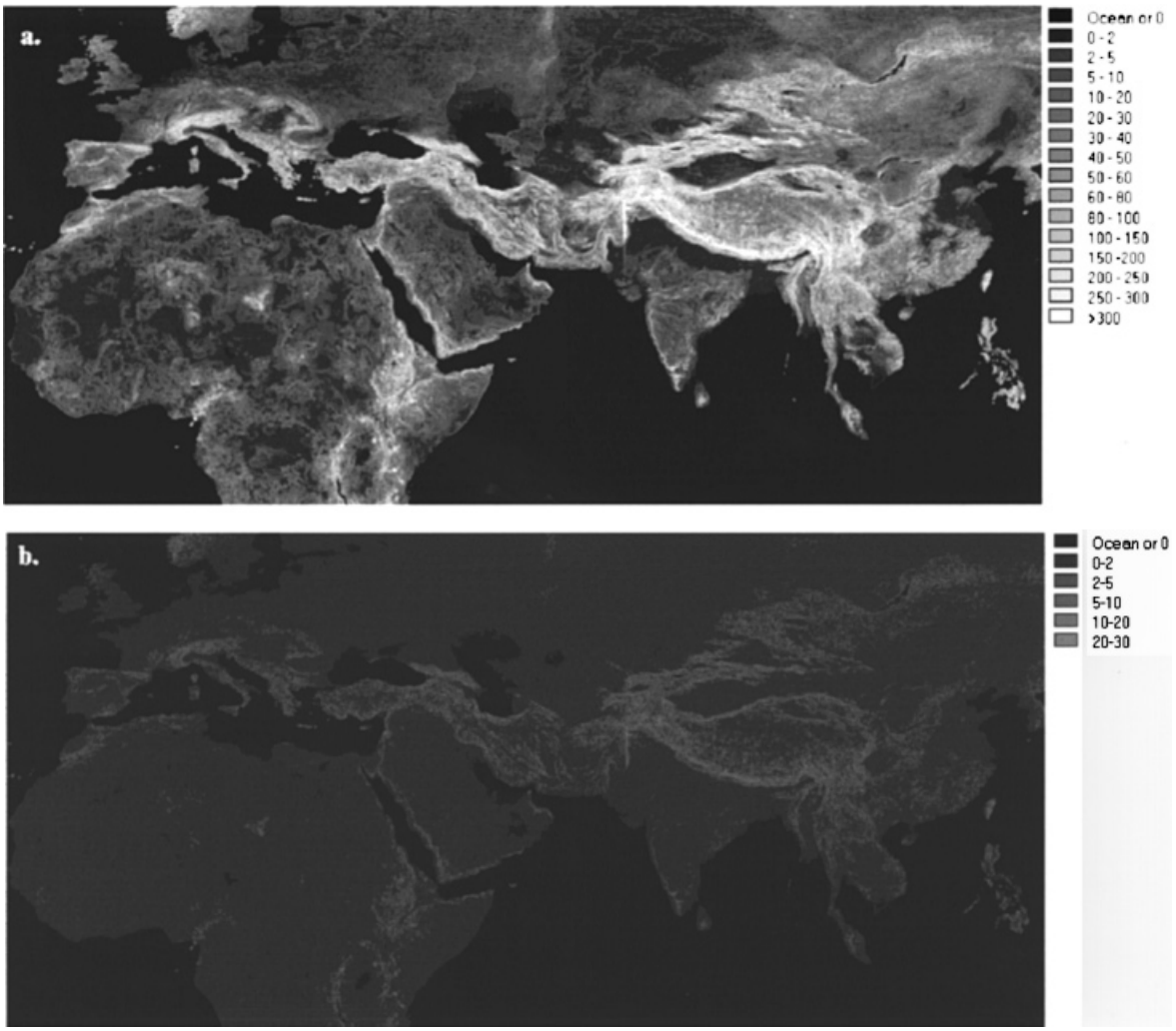

Figure 7. Comparison of unscaled and scaled slope for the Eurasia and northern Africa 5′ DEM: (a) scaled slope derived from the 5′ DEM using $d = 30$ m; (b) unscaled slope derived directly from the 5′ DEM. Note the loss of detail at the same scale using the coarse resolution slope estimates

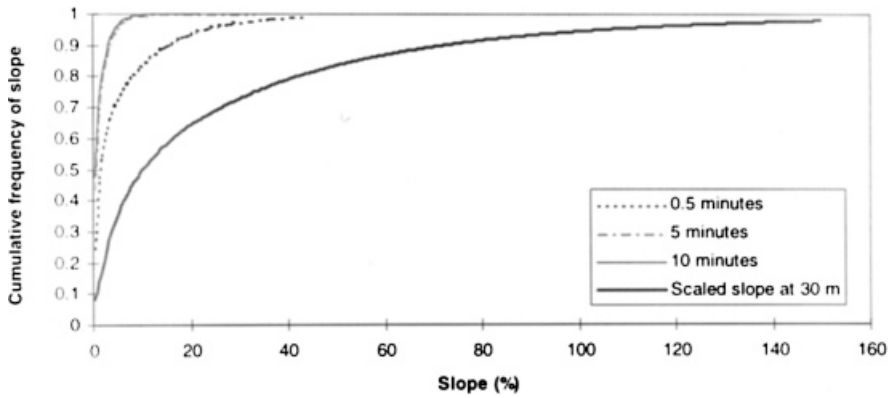

Figure 8. Cumulative frequency distribution of estimated slope at different scales for the Eurasia and northern Africa DEM

Changes in the scale of a DEM have a much larger effect on the slope than the different methods of calculating slope. As the resolution becomes coarser the slopes get lower, whichever method of slope calculation is used. Although the slope is reduced significantly in large scale DEMs, our analysis of multiple scale DEMs shows three significant features. First, the standard deviation of elevation is very stable in a specified area at each DEM resolution. Secondly, as would be expected on theoretical grounds, the local fractal dimension of topography approximates to unity for a completely smooth surface and to two for very irregular surfaces. This fact implies that different kinds of terrain have characteristically different textures that can be expressed in terms of variations in the fractal dimension (Klinkenberg, 1992). Furthermore, the coefficient α varies from 0 to 10^4 over the same area, and is also a good indicator of topographic variation. Thirdly, there are significant relationships between topographic fractal parameters and the standard deviation of elevation. Thus the standard deviation can be used to predict the fractal dimension D and fractal coefficient α.

We have shown that these fractal parameters can then be used to estimate the slope at a specified finer scale from the coarse resolution DEMs. The resultant scaled slope has good statistical properties in most areas although scaled slopes are affected where elevations change rapidly. This occurs in about 4–6 per cent of the subareas when the pixel size of the coarse DEMs is more than 32 times larger than that in the high resolution DEMs. Validation of this method shows that the scaled slope values are very similar to the high resolution slope values in both the Guadalentín Basin and in the Guadalfeo Basin DEMs. Comparing the slopes produced from DEMs at 30″, 5′ and 10′ to those of the scaled slope, it is shown that scaled slope greatly improves the estimation when compared to the slope calculated from the coarse scale DEM.

The finest resolution at which scaled slopes have been validated in this paper is the 30-m resolution. This limit was imposed by the availability of fine resolution data rather than being based on any assumption that it is in any way the 'best' resolution to use. For example, Quinn *et al.* (1991) demonstrated that features of much less than the 50 m resolution are significant in hydrological routing. The importance of microtopographic features in overland-flow routing was also suggested by Parsons *et al.* (1997), who used a DEM with a 0·5 m pixel size. From this perspective, the optimal resolution would be the highest resolution available, with a necessary compromise because of limitations on the size of the DEM and the computer time required to analyse it. If the global topography were unifractal, then the results presented here suggest that as spatial resolution increases, the average slope increases to approach infinity. Such a situation would clearly be impractical to deal with. However, the high variability of the fractal coefficient and dimension demonstrated here suggests that topography has multifractal characteristics. The analysis of high resolution laser altimetry data (Pachepsky and Ritchie, 1998) as well as of microtopographic data (J. Wainwright, A. J. Parsons and A. D. Abrahams, unpublished data) support this suggestion, and imply that it may be possible to use multifractal techniques to define the optimal resolutions required in different modelling studies. Further work into these techniques is currently underway.

ACKNOWLEDGEMENTS

We would like to express our grateful thanks to Professor Michael F. Goodchild and two anonymous referees for providing valuable suggestions and comments on an earlier draft of this manuscript. The opinions expressed above, however, do not necessarily coincide with those of the referees. Thanks are also due to MEDALUS group in the University of Leeds for the use of the Guadalentín Basin DEM, the National Centre of Geographical Information in Spain for the use of the Guadalfeo Basin DEM, and Gabriel Del Bario and Corinna Hawkes for the DEM data of the Rambla del Chortal. We thank Peter Howard for help in the production of the figures.

REFERENCES

Andrle, R. and Abrahams, A. D. 1989. 'Fractal techniques and the surface roughness of talus slopes', *Earth Surface Processes and Landforms*, **14**, 197–209.

Aviles, C. A., Scholz, C. H. and Boatwright, J. 1987. 'Fractal analysis applied to characteristic segments of San Andreas fault', *Journal of Geophysical Research*, **92**(**B1**), 331–334.

Band, L. E. 1986. 'Topographic partition of watersheds with digital elevation models', *Water Resources Research*, **22**, 15–24.
Band, L. E. and Moore, I. D. 1995. 'Scale: landscape attributes and Geographical Information Systems', in Kalma, J. D. and Sivapalan, M. (Eds), Scale Issues in Hydrological Modelling, John Wiley, Chichester, 159–180.
Barenblatt, G. I., Zhivago, A. V., Neprochnov, Y. P. and Ostrovskiy, A. A. 1984. 'The fractal dimension: A quantitative characteristic of ocean-bottom relief', *Oceanology*, **24**, 695–697.
Beven, K. J. and Kirkby, M. J. 1979. 'A physically based, variable contributing area model of basin hydrology', *Hydrological Sciences Bulletin*, **24**(**1**), 43–69.
Cressie, N. and Hawkins, D. M. 1980. 'Robust estimation of the variogram: I', *Mathematical Geology*, **12**, 115–125.
De Jong, S. M. and Burrough, P. A. 1995. 'A fractal approach to the classification of Mediterranean vegetation types in remotely sensed images', *Photogrammetric Engineering and Remote Sensing*, **61**(**8**), 1041–1053.
Drake, N. A., Vafeidis, A., Wainwright, J. and Zhang, X. 1995. 'Modelling soil erosion using remote sensing and GIS techniques', Proceedings of RSS 95 Remote Sensing in Action, 11–14 September 1995, Southampton, 217–224.
Evans, I. S. 1980. 'An integrated system of terrain analysis and slope mapping', *Zeitschrift für Geomorphologie, N.F. Supplementband*, **36**, 274–295.
Fox, C. G. and Hayes, D. E. 1985. 'Quantitative methods for analysing the roughness of the seafloor', *Reviews of Geophysics*, **23**(**1**), 1–48.
Goodchild, M. F. 1982. 'The fractional Brownian process as a terrain simulation model', *Modelling and Simulation*, **13**, 1133–1137.
Håkanson, L. 1978. 'The length of closed geomorphic lines', *Mathematical Geology*, **10**, 141–167.
Hammer, R. D., Young, F. J., Wollenhaupt, N. C., Barney, T. L. and Haithcoate, T. W. 1995. 'Slope class maps from soil survey and digital elevation models', *Soil Science Society of America Journal*, **59**(2), 509–519.
Helmlinger, K. R., Kumar, P. and Foufoula-Georgiou, E. 1993. 'On the use of digital elevation model data for Hortonian and fractal analyses of channel networks', *Water Resources Research*, **29**(8), 2599–2613.
Horn, B. K. P. 1981. 'Hill shading and reflectance map', *Proceedings of the IEEE*, **69**(1), 14–47.
Huang, J. and Turcotte, D. L. 1989. 'Fractal mapping of digitized images: application to the topography of Arizona and comparisons with synthetic images', *Journal of Geophysical Research*, **94**(B6), 7491–7495.
Jones, K. H. 1996. 'A comparison of eight algorithms used to compute slopes as a local property of the DEM', Proceedings of the GIS Research UK 1996 Conference, 7–12.
Kent, C. and Wong, J. 1982. 'An index of littoral zone complexity and its measurement', *Canadian Journal of Fisheries and Aquatic Sciences*, **39**, 847–853.
Klinkenberg, B. 1992. 'Fractals and morphometric measures: Is there a relationship?', *Geomorphology*, **5**, 5–20.
Klinkenberg, B. and Goodchild, M. F. 1992. 'The fractal properties of topography: a comparison of methods', *Earth Surface Processes and Landforms*, **17**(3), 217–234.
Mandebrot, B. B. 1982. The Fractal Geometry of Nature. Freeman, New York.
Montgomery, D. R. and Foufoula-Georgiou, E. 1993. 'Channel network source representation using digital elevation models', *Water Resources Research*, **29**(12), 3925–3934.
Moore, I. D., Grayson, R. B. and Landson, A. R. 1993. 'Digital terrain modelling: a review of hydrological, geomorphological, and biological applications', in Beven, K. J. and Moore, I. D. (Eds), Terrain Analysis and Distributed Modelling in Hydrology, John Wiley, Chichester, 7–34.
Morris, D. G. and Heerdegen, G. 1988. 'Automatically derived catchment boundaries and channel networks and their hydrological applications', *Geomorphology*, **1**, 131–141.
Pachepsky, Y. A. and Ritchie, J. C. 1998. 'Seasonal changes in fractal landscape surface roughness estimated from airborne laser altimetry data', *International Journal of Remote Sensing*, **19**(13), 2509–2516.
Parsons, A. J., Wainwright, J., Abrahams, A. D. and Simanton, J. R. 1997. 'Distributed dynamic modelling of interrill overland flow', *Hydrological Processes*, **11**(14), 1833–1859.
Quinn, P., Beven, K., Chevallier, P. and Planchon, O. 1991. 'The prediction of hillslope flow paths for distributed hydrological modelling using digital terrain models', *Hydrological Processes*, **5**, 59–79.
Russ, J. C. 1993. Fractal Surfaces, Plenum Press, New York.
Shelberg, M. C., Moellering, H. and Lam, N. S. 1982. 'Measuring the fractal dimensions of empirical cartographic curves', Proceedings: Auto-Carto, 5, 481–490.
Skidmore, A. K. 1989. 'A comparison of techniques for calculating gradient and aspect from a gridded digital elevation model', *International Journal of Geographical Information Systems*, **3**(4), 323–334.
Smith, T. R. Zhan, C. and Gao, P. 1990. 'A knowledge-based, two-step procedure for extracting channel networks from noisy DEM data', *Computer Geoscience*, **16**, 777–786.
Travis, M. R., Elsner, G. H., Iverson, W. D. and Johnson, C. G. 1975. 'VIEWIT computation of seen areas, slope and aspect for land-use planning', US Department of Agriculture Forest Service Gen. Techn. PSW 11/1975, Pacific Southwest Forest and Range Experimental Station, Berkley, California, USA.
Turcotte, D. L. 1992. Fractals and Chaos in Geology and Geophysics, Cambridge University Press, Cambridge.
Zevenbergen, L. W. and Thorne, C. 1987. 'Quantitative analysis of land surface topography', *Earth Surface Processes and Landforms*, **12**, 47–56.
Zhang, W. and Montgomery, D. R. 1994. 'Digital elevation model grid size, landscape representation, and hydrologic simulations', *Water Resources Research*, **30**(4), 1019–1028.
Zhang, X., Drake, N. A., Wainwright, J. and Mulligan, M. 1997. 'Global scale overland flow and soil erosion modelling using remote sensing and GIS techniques: model implementation and scaling', Proceedings of RSS '97 Remote Sensing in Action, 2–4 September 1997, Reading, 379–384.

